XL CILAMCE
IBERO-LATIN AMERICAN CONGRESS ON COMPUTATIONAL METHODS IN ENGINEERING
NOVEMBER 11-14, 2019
Praiamar Natal Hotel & Convention
Natal, RN-BRAZIL

A TOPOLOGY OPTIMIZATION METHOD APPLIED TO SUBSEA STRUCTURES UNDER SIMULTANEOUS THERMAL EXPANSION AND HYDROSTATIC PRESSURE LOADS

Renato Picelli
rpicelli@usp.br
Department of Mining and Petroleum Engineering, University of São Paulo
Praça Narciso de Andrade, Vila Mathias, Santos - SP, 11013-560, Brazil
Raghavendra Sivapuram
rsivapur@eng.ucsd.edu
Structural Engineering Department, University of California, San Diego
9500 Gilman Drive, San Diego, CA 92093, USA

Abstract. The effect of severe environmental conditions, i.e., high pressure and high temperature (HPHT), is known to cause various difficulties for the design of deepwater structures for oil and gas production [1]. Subsea structures can be difficult to be repaired and/or replaced in response to the occurrence of unexpected problems due to severe HPHT conditions. Therefore, several methods have been developed to design structures to withstand simultaneous pressure and thermal expansion [2]. This paper aims to propose a topology optimization method to handle the challenges that simultaneous hydrostatic pressure and thermal expansion impose on structural design. Topology optimization methods aim to find optimal material distribution layouts (topologies) on specified design domains minimizing or maximizing an objective function subject to a set of constraints. The structural topologies are usually organic and non-intuitive designs and they represent a powerful computational tool in the early stage of the structural design. Herein, the proposed Topology Optimization of Binary Structures (TOBS) method [3] uses discrete 0,1 design variables within a finite element mesh to indicate the existence of solid 1 and void 0 material inside the design domain. A fluid pressure field is solved with a separate domain and constant thermal expansion is applied on the structural volume. Sequential integer linear programming is used to solve the optimization problem iteratively. The discrete nature of the method presents attractive features when dealing with design dependent body and surface loads. In this paper, we use the structural mean compliance and volume as functions for optimization. The methods of topology optimization have achieved industrial maturity to be applied in stiffness maximization problems, but they are still quite limited when it comes to Multiphysics design. A numerical example of a subsea structural design is explored in this paper.

Keywords: Structural Optimization; Topology Optimization; Subsea Structures; Fluid Pressure; Thermal Expansion;

1 Introduction

For the deepwater development of oil and gas production, it is well recognized that the effect of severe environmental conditions, i.e., high pressure and high temperature (HPHT), has caused various difficulties [1]. Recently, several researches have proposed designs for robust offshore and subsea structures that can withstand the above mentioned problems [2]. In HPHT conditions, thermal expansion naturally occurs in structures such as pipelines, subsea systems, and topside facilities. Therefore, engineers must carefully design and confirm the robustness of offshore oil and gas production structures. This is especially true for subsea structures that are difficult to repair and/or replace in response to the occurrence of unexpected problems, the cost of which is much greater than those of onshore or nearshore cases.

To overcome HPHT-related problems of subsea pipelines, i.e., thermal expansion and global and local deformation, engineers must consider the amount of thermal expansion that may take place. Several methods have been proposed in order to predict the effects of structures under HPHT conditions [2]. Optimization methods represent a potential tool to overcome structural failure in these cases as the complexity of the physics increases. This work proposes to investigate the applications of a specific class of structural optimization methods, namely topology optimization, to subsea structures under hydrostatic pressure and thermal expansion loads.

Structural topology optimization is an intense research field. The idea of the method is to find the optimal material distribution inside a design domain that minimizes a cost function subject to prescribed constraints. The future perspectives pointed out in the survey by Deaton and Grandhi [4] are still target of research. One of them is referred as *design-dependent physics*. In such problems, the interaction between two or more physics depends on the material distribution and its boundaries, i.e., the structural design itself. In such scenario, hydrostatic fluid pressure and thermal expansion lead to design-dependent loads. Therefore, the applications of topology optimization in the offshore systems are still limited.

Thermal expansion loads depend on the volume the structure occupies. This is a partially unresolved a topic for topology optimization as the loads directly depend on the structural layout. The work by Deaton and Grandhi [5] shows that the current methods can lead to ill-behaved optimization problems and produce solutions that are opposed to engineering practices related to thermal stresses. Also, the competing behavior between the volume objective, the mechanical and the thermal loads, poses additional challenges to the problem formulation. Less material can imply in less compliance due thermal expansion forces and, depending on the boundary conditions, less deformation, whilst more volume always leads to less compliance due to mechanical loading [6]. Hydrostatic fluid pressure also imposes some challenges to structural topology optimization [7]. During optimization, the fluid physics occupies the regions where structural material is removed, which modifies the position of the fluid-structure interfaces. Therefore, the pressure loads can change their location, direction and even magnitude during optimization [8, 9].

This work proposes the use of topology optimization methods with clear definition of structural volume and boundaries. Herein, we apply the Topology Optimization of Binary Structures (TOBS) method, recently created by Sivapuram and Picelli [3], Sivapuram et al. [10], to withstand hydrostatic pressure and thermal expansion loads. In contrast with the classic Solid Isotropic Material with Penalization (SIMP) approach [11] that presents gray areas and fuzzy boundaries due to intermediate densities, the TOBS method restricts the optimization with discrete $\{0, 1\}$ design variables, 1 meaning the presence of a solid material and 0 representing the void regions. This implies that one always explicitly know the volume and surfaces of the structure during optimization. In this case, the application of thermal expansion and pressure loads is straightforward.

The remainder of the paper is organized as follows. Section 2 describes the TOBS. Section 3 describes the finite element formulations used in this work. The optimization problem and sensitivity analysis are described in Section 4. Section 5 shows the application of the method in solving a structural design problem with the presence of thermal and pressure loads. Section 6 summarizes the paper.

2 The Topology Optimization of Binary Structures Method

The structure is discretized into a finite element mesh and for each element a binary density variable $\rho_e \in \{0, 1\}$ is assigned, 0 indicating the absence and 1 the presence of material. A generic binary optimization problem with inequality constraints is given by

$$\begin{aligned} &\underset{\boldsymbol{x}}{\text{Minimize}}\ f(\boldsymbol{x}) \\ &\text{Subject to}\ g_i(\boldsymbol{x}) \leq \overline{g}_i,\ i \in [1, N_g] \\ &\qquad\qquad x_j \in \{0, 1\},\ j \in [1, N_d] \end{aligned} \tag{1}$$

where $\boldsymbol{x}$ is the vector of design variables (densities in case of topology optimization) of size N_d, f is the objective function, g_i is the i^{th} inequality constraint, $\overline{g}_i$ is the associated upper bound, and N_g is the number of inequality constraints. An approximate linearized version of the optimization problem from Eq. (11) is solved at every iteration k. Such linearized problem is given by

$$\begin{aligned} &\underset{\Delta\boldsymbol{x}^k}{\text{Minimize}}\ \frac{\partial f(\boldsymbol{x}^k)}{\partial \boldsymbol{x}} \cdot \Delta\boldsymbol{x}^k \\ &\text{Subject to}\ \frac{\partial g_i(\boldsymbol{x}^k)}{\partial \boldsymbol{x}} \cdot \Delta\boldsymbol{x}^k \leq \overline{g}_i - g(\boldsymbol{x}^k) = \Delta g_i^k,\ i \in [1, N_g] \\ &\qquad\qquad ||\Delta\boldsymbol{x}^k||_1 \leq \beta N_d \\ &\qquad\qquad \Delta x_j^k \in \{-x_j^k, 1 - x_j^k\},\ j \in [1, N_d] \end{aligned} \tag{2}$$

where $(\cdot)^k$ indicates the value of quantity $(\cdot)$ at iteration k, $\Delta\boldsymbol{x}^k$ is the update values of design variables and Δg_i^k is the upper bound of constraint i. An extra constraint based on the 1-norm of design variables is added to restrict the number of flips from 0 to 1, and vice-versa, therefore avoiding dramatic changes in the structural topology from one iteration to another.

The upper bounds of constraints Δg_i^k are modified so that the linearized suboptimization problems yield feasible solutions. The constraint bounds are modified using

$$\Delta g_i^k = \begin{cases} -\epsilon_1 g_i(\boldsymbol{x}^k) & : \overline{g}_i < (1 - \epsilon_1) g_i(\boldsymbol{x}^k) \\ \overline{g}_i - g_i(\boldsymbol{x}^k) & : \overline{g}_i \in [(1 - \epsilon_1) g(\boldsymbol{x}^k), (1 + \epsilon_2) g(\boldsymbol{x}^k)] \\ \epsilon_2 g_i(\boldsymbol{x}^k) & : \overline{g}_i < (1 + \epsilon_2) g_i(\boldsymbol{x}^k) \end{cases} \tag{3}$$

where ϵ_1 and ϵ_2 are parameters chosen from numerical experience. These parameters are selected such that the suboptimization problems obtained through linearization yield feasible solutions. In this work, we used $\epsilon_1 = \epsilon_2 = \epsilon$ for simplicity.

The integer suboptimization problems generated using sequential linearization can be solved using Integer Linear Programming (ILP). In this work, the ILP problem is solved using the branch-and-bound method of CPLEX package. The CPLEX package includes the `cplexmilp` function which solves mixed integer linear problems. The branch-and-bound method is an algorithm based on the heap data structure. The TOBS framework using branch-and-bound method successfully demonstrated in [10] some problems using up to 6 constraints. The derivatives in the linearized subproblems are called sensitivities of the objective function f and constraint functions g_i. In the context of topology optimization, a Finite Element Analysis (FEA) is performed for each set of design variables to compute the sensitivities. A MATLAB implementation of this method is available at `https://github.com/renatopicelli/tobs`.

3 Finite Element Analysis

3.1 Structural Problem

Consider a linear elastostatics problem with external mechanical loads and thermal loads (through uniform temperature change) acting on a structural domain Ω,

$\sigma_{ij,j} + b_i = 0$	Equilibrium
$\sigma_{ij} = D_{ijkl}(\epsilon_{kl} - \alpha \Delta T \delta_{kl})$	Constitutive Equation
$\epsilon_{kl} = u_{(k,l)}$	Kinematic Compatibility
$u = g$ for $\boldsymbol{x} \in \Gamma_g$	Essential Boundary Conditions
$\sigma_{ij} n_j = t_i$ for $\boldsymbol{x} \in \Gamma_t$	Natural Boundary Conditions
$u_i : \Omega \to \mathbb{R}$	Solution Map

Table 1. Strong Form for linear elastostatics

where σ is the stress field, b is the body load, D is the elasticity tensor, ϵ is the strain field, α is the coefficient of thermal expansion, ΔT is the uniform temperature change, $(\cdot)_{(k,l)}$ is the symmetric gradient, u is the displacement field, g is the specified displacement field, $\boldsymbol{x}$ is the coordinate, Γ_g is the part of the boundary where displacement is specified, n_j is the normal vector, t_i is the traction loading and Γ_t is the traction loaded boundary. The finite element approximation on the variational form (n_{el} elements and n_{nd} nodes) yields

Find $\boldsymbol{u}^h = \{\boldsymbol{u}^h : \boldsymbol{u}^h \in \mathcal{S}^h \subset \mathcal{S}$ and $\boldsymbol{u}^h = \boldsymbol{g}^h$ for $\boldsymbol{x} \in \Gamma_g\}$ such that

$$\int_\Omega \delta \boldsymbol{u}^{h^T} \boldsymbol{B}^{s^T} \boldsymbol{D} \boldsymbol{B}^s \boldsymbol{u}^h \, d\Omega = \int_\Omega \delta \boldsymbol{u}^{h^T} \boldsymbol{N}^{s^T} \boldsymbol{b} \, d\Omega + \int_{\Gamma_t} \delta \boldsymbol{u}^{h^T} \boldsymbol{N}^{s^T} \boldsymbol{N}^s \boldsymbol{t}^h \, d\Omega + \int_\Omega \alpha \Delta T \delta \boldsymbol{u}^{h^T} \boldsymbol{B}^{s^T} \boldsymbol{D} \boldsymbol{q} \, d\Omega \tag{4}$$

where $\mathcal{S}$ is the solution space for displacements, $\boldsymbol{u}$ and $\boldsymbol{g}$ represent the displacement vector and specified displacement vector respectively at a material coordinate, the superscript $(\cdot)^h$ indicates that the quantity $(\cdot)$ is discretized, h indicates the element size, $\boldsymbol{u}^h$ is the vector of nodal displacements, $\mathcal{S}^h$ is the finite element approximation space, $\boldsymbol{N}^s$ and $\boldsymbol{B}^s$ are the matrices corresponding to shape functions and their gradients respectively. The vector $\boldsymbol{q}$ is given by $[1, 1, 0]^T$ for 2D problems. The matrix form of the present linear elastostatics problem is

$$\boldsymbol{K}\boldsymbol{u} = \boldsymbol{F}^{mech} + \boldsymbol{F}^{th} \tag{5}$$

where $\boldsymbol{K}$ is the stiffness matrix (corresponding to the left hand side of (4)), $\boldsymbol{F}^{mech}$ and $\boldsymbol{F}^{th}$ are the mechanical and thermal loading respectively. $\boldsymbol{F}^{th}$ corresponds from the third term of the right hand side of (4), and $\boldsymbol{F}^{mech}$ corresponds to the first two terms. The stiffness matrix and load vectors are obtained by assembly of element-wise matrices.

3.2 Fluid Problem

The physics of the fluid used in this work is governed by the Laplacian equation for pressure,

$\nabla^2 p = 0$	Laplacian
$p = p_0$ for $\boldsymbol{x} \in \Theta_g$	Essential Boundary Conditions
$p_{,i} n_i = r_i$ for $\boldsymbol{x} \in \Theta_r$	Natural Boundary Conditions
$p : \Pi \to \mathbb{R}$	Solution Map

Table 2. Strong form for the fluid problem

where p is the pressure, Π is the fluid domain, Θ_g is the part of the boundary with specified pressures, Θ_r is the source boundary, n_i is the normal to the fluid domain and r_i is the source field. Upon finite element discretization, the Galerkin form of the governing equation can be obtained as

$$\begin{gathered}\text{Find } \boldsymbol{p}^h = \{\boldsymbol{p}^h \in \mathcal{P}^h \subset \mathcal{P},\ p = p_0 \text{ for } \boldsymbol{x} \in \Theta_g\} \text{ such that} \\ \int_\Pi \delta \boldsymbol{p}^{h^T} \boldsymbol{B}^{f^T} \boldsymbol{B}^f \boldsymbol{p}^h \, d\Pi = \int_{\Theta_r} \delta \boldsymbol{p}^h \boldsymbol{N}^{f^T} \boldsymbol{N}^f \boldsymbol{r} \, d\Theta\end{gathered} \tag{6}$$

where $\mathcal{P}$ is the feasible space of pressures, the superscript $(\cdot)^h$ is the discretized field, $\boldsymbol{r}$ is the discretized source field, $\boldsymbol{N}^f$ and $\boldsymbol{B}^f$ are the shape function and shape function gradients corresponding to the fluid domain. The matrix form for pressure equations can be written as

$$\boldsymbol{K}^f \boldsymbol{p} = \boldsymbol{F}^f \tag{7}$$

where $\boldsymbol{K}^f$ and $\boldsymbol{F}^f$ are the system matrix/vector for pressure equations, and are obtained by the assembly of element-based matrix/vector.

3.3 Fluid-Structure Coupling

In this work, we use zero source and traction natural boundary conditions on, respectively, Θ_r for the fluid problem and Γ_t for the structural problem, and no body loading for the structure (i.e., $b = 0$). At the fluid-structure interface Γ_{fs}, the pressure field of the fluid acts as the traction field on the structure. The fluid-structure coupling is achieved by using the boundary condition

$$\sigma_{ij} n_j = -p n_i \text{ for } \boldsymbol{x} \in \Gamma_{fs} \tag{8}$$

Including the coupling boundary conditions, the coupled system of equations to be solved are

$$\begin{pmatrix} \boldsymbol{K}^s & -\boldsymbol{L}^{fs} \\ \boldsymbol{0} & \boldsymbol{K}^f \end{pmatrix} \begin{bmatrix} \boldsymbol{u} \\ \boldsymbol{p} \end{bmatrix} = \begin{bmatrix} \boldsymbol{F}^{th} \\ \boldsymbol{0} \end{bmatrix} \tag{9}$$

where $\boldsymbol{L}^{fs}$ is the fluid-structure coupling matrix, given by

$$\boldsymbol{L}^{fs} = \int_{\Gamma_{fs}} \boldsymbol{N}^{s^T} \boldsymbol{n} \boldsymbol{N}^f \, d\Gamma \tag{10}$$

This system of equations is coupled only one-way: from fluid to structure. The fluid pressures can first be calculated and traction loads can be applied on the structure to enable solving the structural problem. For a fully coupled system, the $\boldsymbol{0}$ in the system of equations would be nontrivial. So, this system of equations can serve as a good starting point for the analysis of fluid-structure systems.

4 Optimization Problem and Sensitivity Analysis

In this work, topology optimization is applied aiming to design the stiffest structure given a volumetric material usage constraint. To maximize stiffness is equivalent to minimize the structural compliance C. This optimization problem can be written as

$$\begin{aligned} &\underset{\boldsymbol{x}}{\text{Minimize}}\ C(\boldsymbol{x}) \\ &\text{Subject to}\ V(\boldsymbol{x}) \leq \overline{V} \\ &\qquad\quad x_j \in \{0,1\},\ j \in [1, N_d] \end{aligned} \tag{11}$$

where $V(\boldsymbol{x})$ is the volume fraction of the structural topology, $\overline{V}$ is the constrained volume fraction and N_d is the number of design variables. The compliance of a structure is defined using the mean strain energy as

$$C(\boldsymbol{x}) = \frac{1}{2}\boldsymbol{u}^T\boldsymbol{K}^s\boldsymbol{u} \tag{12}$$

The displacements $\boldsymbol{u}$ are computed using the coupled system of equations in (9).

As shown in Sec. 2, the topology optimization problem requires the gradients (sensitivities) of the associated objective and constraint functions to iterate over solutions. The sensitivities for the present compliance function with respect to the design variables (structural finite elements) are expressed as

$$\frac{\partial C}{\partial x_j} = -\frac{1}{2}\boldsymbol{u}_e^T\frac{\partial \boldsymbol{K}_e^s}{\partial x_j}\boldsymbol{u}_e + \boldsymbol{u}_e^T\frac{\partial \boldsymbol{F}_e^{th}}{\partial x_j} + \boldsymbol{u}^T\frac{\partial \boldsymbol{L}^{fs}}{\partial x_j}\boldsymbol{p} \tag{13}$$

where the first term gives the compliance sensitivities for a structure without thermal and design-dependent loads, the second term represents the effect of thermal loading on the sensitivities and the third term gives the sensitivities due to design-dependent pressure loads. The sensitivities of the volume fraction function with respect to a design variable e are given by

$$\frac{\partial V}{\partial x_j} = V_e \tag{14}$$

where V_e is the area (in 2D) of the finite element e.

To avoid checkerboard solutions (a common problem for topology optimization methods) and noisy sensitivities, a conventional mesh-independent filter is used to produce smooth sensitivity fields. This filter is demonstrated to yield mesh-independent and non-checkerboard solutions ([3], [12]). A nodal sensitivity field is first computed using averages of sensitivities corresponding to the connected finite elements. The nodal sensitivities are computed as

$$\frac{\partial f}{\partial y_n} = \frac{1}{|E|}\sum_{e\in E}\frac{\partial f}{\partial x_j} \tag{15}$$

where f is a generic function, y_n is a virtual nodal design variable, E is the set of elements surrounding node n and $|E|$ is the cardinality of set E. The filtered element-based sensitivities of an element e is obtained from the nodal sensitivity field using weighted average over a neighborhood of the finite element e. The filtered sensitivity field is given as

$$\frac{\partial f}{\partial x_j} = \frac{\sum_{m\in N} w_{nm}\dfrac{\partial f}{\partial y_m}}{\sum_{m\in N} w_{nm}} \tag{16}$$

where $\dfrac{\partial f}{\partial \rho_e}$ is the filtered element-based sensitivity and N is the neighborhood around element e.

5 Numerical Examples

We consider the example of a biclamped beam ($l \times b = 0.15 \times 1$ m^2) in contact with a fluid field. This could be interpreted as the design problem of the cross-section of a pipe or subsea mechanical system under pressure and thermal loads. The structure is discretized using 400×60 bilinear quadrilateral elements. Plane stress is assumed. The beam is made of a material with Young's modulus $E = 199.5$ GPa, Poisson's ratio $\nu = 0.3$ and coefficient of thermal expansion $\alpha = 15.4 \times 10^6$ °C^{-1}. The beam is clamped at both the ends. The fluid above the structure carries a varying pressure field, with essential boundary conditions $P_{in} = 10$ MPa and $P_{out} = 1$ MPa. The investigation is done for different thermal loads, i.e., uniform temperature difference ΔT values.

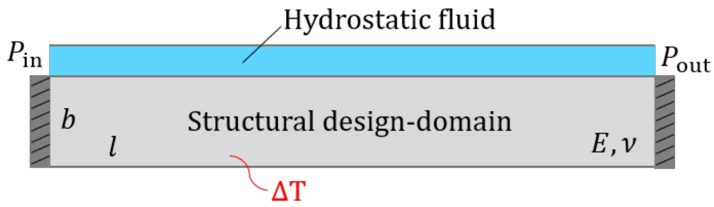

Figure 1. Structural design problem.

For an initial full solid design, Fig. 2(a) presents the scaled plot of the structural displacement field when only the hydrostatic pressure loads are acting. Figure 2(b) and (c) show the thermal expansion of the structure when subject to, respectively, positive and negative temperature difference. The deformations of the structure under these separate load cases are quite different between each other and their combination can considerably affect the optimization. The direction of the displaced structural regions are also different, depending on the load case, which can lead to the addition or cancellation of loads when combined. The structural mean compliance value for each load case is indicated in Fig. 2.

In order to investigate the combination of the pressure and thermal expansion loads, the structure is subject to optimization. The volume fraction of the optimization problem is 0.5, and the parameters used are $\beta = 0.05$, $\epsilon = 0.01$ and $r = 0.02$m. In all the cases, the initial solution used is the fully-solid design. First, it is considered that the fluid-structure interface can not change its location, i.e., the structural elements close to the fluid are considered as non-design domain. Figure 3 presents the optimized topologies when the structure is subject to the hydrostatic pressure loads and three different temperature changes, $\Delta T = 0$°C, $\Delta T = 2.5$°C and $\Delta T = -2.5$°C. It can be observed that the combination of the hydrostatic pressure loads with the positive thermal expansion ($\Delta T = 2.5$°C) caused a more significant change in the optimized structure. In this case, the members in the bottom of the structure disappeared if compared to the case with $\Delta T = 0$°C. The deformation of the structure under $\Delta T = 2.5$°C increases the stresses in the bottom region, consequently, it is interesting to remove that part of the structure. This information is transferred out to the optimizer via the thermal expansion term in the sensitivity equation from Eq. (13). When applying a $\Delta T = -2.5$°C, the critical stresses are in the top region of the structure, however, they can not be removed in this example and the structure must support them with the bars present in the optimized topology. The mean compliance value for the optimized structures are indicated in Fig. 3.

The next example considers the case where the fluid-structure interface can change its location. This implies in a much more challenging problem for topology optimization, classified as design-dependent, since the surface and volumetric loads also change [13]. Figure 4 presents the optimized structures, and mean compliance values, considering the hydrostatic pressure load and different positive ΔT's when allowing the interfaces to change. In this case, the patterns in the optimized topologies are similar to the ones with fixed interface. Material is removed from the bottom regions of the structure, but then adjusting the fluid-structure surfaces to support the hydrostatic pressure with an arch-like structure. It is also important to point out that the mean compliance values for the optimized structures with changing interfaces are generally lower than the ones where the interfaces are kept fixed.

The optimized structure solved when the thermal expansion loads arise from a negative temperature difference is shown in Fig. 5. It can be observed that the material in the top region of the structure is removed, as opposed to the case of positive ΔT's. This is because the compression region of the structure is added up by the thermal expansion deformation, becoming more critical. Figure 6(a) and 6(b) present

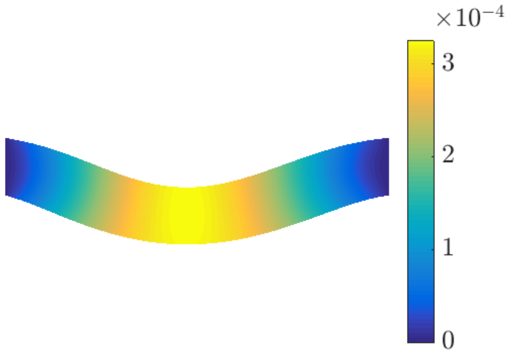

(a) $C(\boldsymbol{x})$ = 516.30 Nm

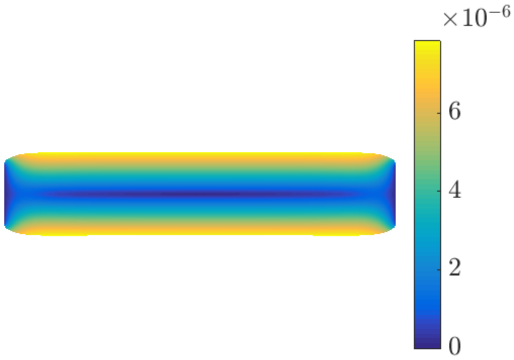

(b) $C(\boldsymbol{x})$ = 169.04 Nm

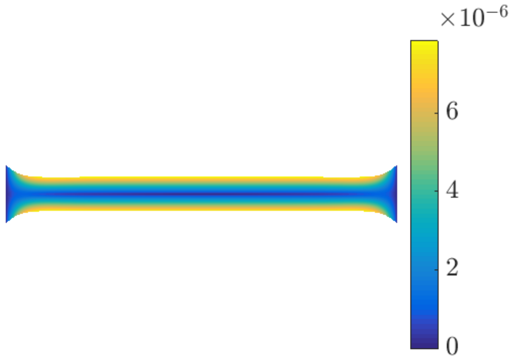

(c) $C(\boldsymbol{x})$ = 169.04 Nm

Figure 2. Structural displacement fields (scaled plots) under separate load cases: (a) pressure loads, (b) thermal expansion under positive temperature difference and (c) thermal expansion under negative temperature difference.

(a) $\Delta T = 0^o$C; $C(\boldsymbol{x})$ = 844.84 Nm

(b) $\Delta T = 2.5^o$C; $C(\boldsymbol{x})$ = 868.06

(c) $\Delta T = -2.5^o$C; $C(\boldsymbol{x})$ = 844.84

Figure 3. Topology optimization of the biclamped beam under the combination of hydrostatic pressure and thermal expansion loads with different ΔT's.

the convergence history of the structural mean compliance and volume fraction functions. The peak on the compliance history indicates the break of a structural member.

(a) $\Delta T = 0^{\text{o}}\text{C}$; $C(\boldsymbol{x})$ = 806.60 Nm

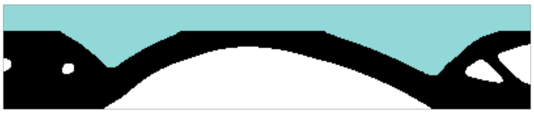

(a) $\Delta T = 2.5^{\text{o}}\text{C}$; $C(\boldsymbol{x})$ = 730.69 Nm

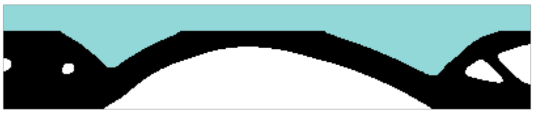

(b) $\Delta T = 5.0^{\text{o}}\text{C}$; $C(\boldsymbol{x})$ = 705.52 Nm

(c) $\Delta T = 7.5^{\text{o}}\text{C}$; $C(\boldsymbol{x})$ = 743.87 Nm

Figure 4. Topology optimization of the biclamped beam under the combination of hydrostatic pressure and thermal expansion loads allowing the fluid-structure interfaces to change location.

$\Delta T = -5.0^{\text{o}}\text{C}$; $C(\boldsymbol{x})$ = 775.23 Nm

Figure 5. Topology optimization of the biclamped beam under the combination of hydrostatic pressure and thermal expansion loads with negative ΔT's considering design-dependency of the fluid-structure interface.

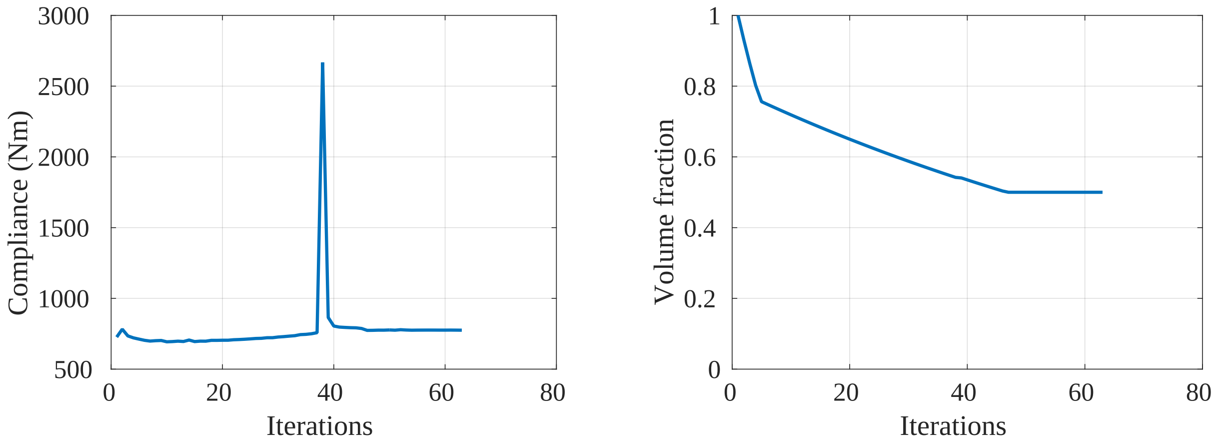

Figure 6. Mean compliance and volume fraction functions convergence history.

6 Conclusions

This paper presented a topology optimization methodology applied to the design of structures under hydrostatic pressure and thermal expansion loads. Applications can include structural design problems in offshore systems. The method employs discrete $\{1, 0\}$ design variables, which allows for the switch between fluid and structural regions straightforwardly. It was shown that hydrostatic pressure and thermal expansion loads can cause very different deformation configurations on the structure when applied separately. This is reflected on the optimization results, which indicate that the combination of both type of loads into a single load case causes the optimized structure to occupy different regions of the design domain. Convergence was achieved smoothly. The method presented here can be considered as one tool for the design of structures under complex multiphysics loads. Future works shall include more detailed analyses and offshore applications.

Acknowledgements

Renato Picelli would like to thank the support of São Paulo Research Foundation (FAPESP), grants 2018/05797-8 and 2019/01685-3.

References

[1] Seo, J. H., Kim, D. K., Choi, H. S., Yu, S. Y., & Park, K. S., 2018. Simplified technique for predicting offshore pipeline expansion. *Journal of Marine Science and Application*, vol. 17, pp. 68–78.

[2] Bai, Q. & Bai, Y., 2014. *Subsea pipelines design, analysis and installation – Part II: pipeline design, chapter*, chapter 9. Gulf Professional Publishing, Oxford.

[3] Sivapuram, R. & Picelli, R., 2018. Topology optimization of binary structures using integer linear programming. *Finite Elements in Analysis and Design*, vol. 139, pp. 49–61.

[4] Deaton, J. D. & Grandhi, R. V., 2014. A survey of structural and multidisciplinary continuum topology optimization: post 2000. *Structural and Multidisciplinary Optimization*, vol. 49, pp. 1–38.

[5] Deaton, J. D. & Grandhi, R. V., 2013. Stiffening of restrained thermal structures via topology optimization. *Structural and Multidisciplinary Optimization*, vol. 48, n. 4, pp. 731–745.

[6] Pedersen, P. & Pedersen, N. L., 2010. Strength optimized designs of thermoelastic structures. *Structural and Multidisciplinary Optimization*, vol. 42, n. 5, pp. 681–691.

[7] Sigmund, O. & Clausen, P. M., 2007. Topology optimization using a mixed formulation: An alternative way to solve pressure load problems. *Computer Methods in Applied Mechanics and Engineering*, vol. 196, pp. 1874–1889.

[8] Chen, B. C. & Kikuchi, N., 2001. Topology optimization with design-dependent loads. *Finite Elements in Analysis and Design*, vol. 37, pp. 57–70.

[9] Picelli, R., Vicente, W. M., & Pavanello, R., 2015. Bi-directional evolutionary structural optimization for design-dependent fluid pressure loading problems. *Engineering Optimization*, vol. 47, n. 10, pp. 1324–1342.

[10] Sivapuram, R., Picelli, R., & Xie, Y. M., 2018. Topology optimization of binary microstructures involving various non-volume constraints. *Computational Materials Science*, vol. 154, pp. 405 – 425.

[11] Bendsøe, M. P. & Sigmund, O., 2003. *Topology Optimization - Theory, Methods and Applications*. Springer Verlag, Berlin Heidelberg.

[12] Huang, X. & Xie, Y. M., 2007. Convergent and mesh-independent solutions for the bi-directional evolutionary structural optimization method. *Finite Elements in Analysis and Design*, vol. 43, pp. 1039–1049.

[13] Picelli, R., Neofytou, A., & Kim, H. A., 2019. Topology optimization for design-dependent hydrostatic pressure loading via the level-set method. *Structural and Multidisciplinary Optimization*, , n. online.